

CrystEngComm

Accepted Manuscript



This is an *Accepted Manuscript*, which has been through the Royal Society of Chemistry peer review process and has been accepted for publication.

Accepted Manuscripts are published online shortly after acceptance, before technical editing, formatting and proof reading. Using this free service, authors can make their results available to the community, in citable form, before we publish the edited article. We will replace this *Accepted Manuscript* with the edited and formatted *Advance Article* as soon as it is available.

You can find more information about *Accepted Manuscripts* in the [Information for Authors](#).

Please note that technical editing may introduce minor changes to the text and/or graphics, which may alter content. The journal's standard [Terms & Conditions](#) and the [Ethical guidelines](#) still apply. In no event shall the Royal Society of Chemistry be held responsible for any errors or omissions in this *Accepted Manuscript* or any consequences arising from the use of any information it contains.

Cite this: DOI: 10.1039/c0xx00000x

www.rsc.org/xxxxxx

ARTICLE TYPE

An insight into carvedilol solid forms: effect of the supramolecular interactions on the dissolution profiles

Livia Deris Prado,^{*a,b} Helvécio Vinícius Antunes Rocha^b, Jackson Antônio Lamounier Camargos Resende^a, Glaucio Braga Ferreira^a, Ana Maria Rangel de Figueiredo Teixeira^a

Received (in XXX, XXX) Xth XXXXXXXXX 20XX, Accepted Xth XXXXXXXXX 20XX
DOI: 10.1039/b000000x

Carvedilol, a β -blocker drug used to treat hypertension, is known to exhibit polymorphism. Thus far, the crystal structure of two polymorphs (I and II) and one hydrate have been reported. In this study, three crystal modifications of carvedilol were obtained from crystallization experiments. The structure of another polymorph (III) was elucidated for the first time and the crystal structure of the hydrate was also determined from single-crystal diffraction data. Carvedilol structures are characterized by variations in their molecular conformations, with different orientations of the carbazole moiety. Further conformational details also differentiate them. Carvedilol structures II, III and hydrate were characterized by thermal and microscopic methods. A higher melting polymorph (III), compared to form II, was identified when crystallized from methanol. This polymorph showed higher intrinsic dissolution rate than polymorph II in hydrochloric acid at pH 1.4 containing sodium lauryl sulfate 0.1% (w/v). Although not expected due to its greater stability, the higher dissolution rate of polymorph III could be explained by the structural features. The dissolution of carvedilol in acid medium is related to its ability to form protonated molecules. DFT calculation with WB97XD functional was carried out for evaluation of the classic and non classic hydrogen bonds between the molecules in carvedilol structures. The energy involved in the intermolecular interactions explains some experimental observations. This result showed the intermolecular interactions influence on the solid-state properties of carvedilol. Moreover, polymorph III exhibit higher dissolution rate than II, showing a great potential for formulation strategies of this poorly water soluble drug.

Introduction

Polymorphism is a theme of much interest to the pharmaceutical industry. This phenomenon can be defined as the ability of the same chemical compound to exist in different crystalline phases with different arrangements of the molecules in the crystal lattice.¹⁻² This is particularly important in development of active pharmaceutical ingredients (APIs) because, in addition to structural differences, the physical and chemical properties of the polymorphs may differ, including dissolution rate, solubility, melting point and physical/chemical stability.³⁻⁴ These properties can remarkably influence in drug processing and drug product performance.⁵ In order to formulate poorly water-soluble APIs, solid forms, such as polymorphs, are being developed. Hence, it is therefore important to control the crystallization of polymorphs to obtain structures with desired properties.⁶⁻⁷ Many methods have been employed to characterize pharmaceutical polymorphs.⁸ The definitive indication of polymorphism is via demonstration of a different crystal structure by single-crystal X-ray diffraction technique. Powder X-ray diffraction may also be used to demonstrate the existence of polymorphs. Other methods, including microscopy, thermal

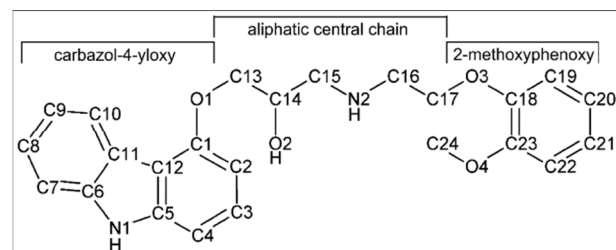


Fig. 1 Molecular structure and fragments of carvedilol.

analysis (e.g. differential scanning calorimetry and thermogravimetric analysis) and spectroscopy (e.g. infrared and Raman) are often used for further characterization of polymorphs.⁹ Carvedilol is an API with multiple actions in the cardiovascular system. It is clinically used for treatment of congestive heart failure, hypertension and myocardial infarction.¹⁰⁻¹¹ The reduction in blood pressure results from β -adrenergic receptor blockade and vasodilatation, the latter resulting from α_1 -adrenergic blocking activity.¹⁰⁻¹² It is administered as a racemic conglomerate of (RS)-1-(9H-carbazol-4-yloxy)-3-[2-(2-methoxyphenoxy)ethylamino] propan-2-ol. The two isomers are equally potent as α_1 -blockers and the S-enantiomer is principally responsible for the β -blockade

activity.¹² Carvedilol is the only β -blocker agent with the presence of the carbazole moiety in their molecule (Fig. 1). The antioxidant activity of carvedilol is attributed to the carbazole moiety.¹¹

The existence of different solid-state forms of carvedilol (polymorphs, hydrate and solvates) has been mentioned in scientific publications, especially in patents.¹³⁻²⁰ Regarding the polymorphism of carvedilol, the crystal structures of two anhydrous modifications were previously reported, I²¹ and II²², both described in space group $P2_1/c$. The crystal structure of the hemihydrate was recently reported.²³

Since the drug is practically insoluble in water²⁴ the existence of different solid-state forms is clearly relevant for drug therapy. Despite the fact that carvedilol is widely approved for the treatment of cardiovascular diseases²⁵, there is little information concerning the crystalline structures of this API. The present study aims a comprehensive understanding of carvedilol crystal forms. We report the crystal structure of one solid modifications of carvedilol, III, which was solved by single-crystal X-ray diffraction technique. A detailed analysis of the crystal packing and conformational features is presented. Besides single-crystal and powder X-ray diffraction methods, we applied thermal and microscopic methods. The dissolution behavior of carvedilol structures II, III and III was studied for the first time. Theoretical studies were carried out to evaluate intermolecular hydrogen bonds in carvedilol forms, allowing the correlation of structural features with their physical properties.

Experimental

Materials

A commercial batch of carvedilol (Indoco Remedies, India) was used without further purification. Several crystallizations from carvedilol raw material were performed under different conditions. All solvents used were analytical grade.

Crystallization Experiments

Crystal structure II was obtained dissolving 1.7 g of carvedilol raw material in 200 mL of toluene by vigorous shaking of the mixture at 60 °C. The newly prepared solution was left standing for 4 days at room temperature. Carvedilol hydrate form was crystallized at room temperature dissolving 300 mg of raw material in 60 mL of ethyl acetate. After solvent evaporation, crystals were collected. The crystal structure III was obtained dissolving 460 mg of carvedilol in 40 mL of methanol. Crystals were collected after 14 days. All samples were dried at reduced pressure. Additional experiments were conducted using various solvent systems, solute concentration and temperature in an effort to obtain different crystal forms of carvedilol.

Powder X-ray Diffraction (PXRD)

PXRD patterns were obtained with a Bruker D8 diffractometer using Cu K α radiation ($\lambda = 1.5418 \text{ \AA}$) with a graphite monochromator. The patterns were recorded at a tube voltage of 40 kV and a tube current of 40 mA, between 3 and 40° in 2θ , with a step size of 0.04° and a scan rate of 3 s. The program MERCURY²⁶ was used for the calculation of the theoretical powder patterns from single-crystal X-ray diffraction data.

X-ray Data Collection and Crystal Structure Determination

The single-crystal X-ray diffraction data were collected at 150 K using Mo K α radiation ($\lambda = 0.71073 \text{ \AA}$) on an Oxford Diffraction Xcalibur Atlas Gemini ultra CCD diffractometer. The crystal structure was solved by direct methods, using the program SHELXS-97.²⁷ SHELXL-97²⁷ was used for least-squares refinements on F^2 . The space group was determined from the systematic absences and their correctness was confirmed by successful solution and refinement of the structures. Anisotropic thermal parameters were refined for all non-hydrogen atoms. The hydrogen atoms were geometrically positioned and refined using a riding model with isotropic displacement parameters based on the isotropic displacement parameter of the attached atom. The geometries of the disordered atoms in the hydrate were restrained to expected values. The programs MERCURY²⁶ and ORTEP-3²⁸ were used to deal with the processed crystallographic data and artwork representation. Crystal data and relevant data collection and refinement are given in Table 1.

Optical Microscopy

Small amounts of samples were spread on glass slides. Images were acquired with a Nikon SMZ800 stereoscopic zoom microscope.

Thermal Analysis

Differential scanning calorimetry (DSC) measurements were performed with a Shimadzu DSC-60 thermal analyzer. DSC curves were recorded by placing precisely weighed quantities (3-3.5 mg) in sealed 34 μ L aluminum pans. The curves were obtained under nitrogen flow rate of 50 mL/min at a heating rate of 10 °C/min, from ambient temperature to 200 °C. Thermogravimetric analysis (TGA) was carried out under the same temperature and atmospheric conditions on a Shimadzu DTG-60 thermal analyzer. The samples were weighed (approximately 5 mg) in 34 μ L aluminum pans.

Powder and Intrinsic Dissolution Tests

The powder and intrinsic dissolution profiles were determined at 37 °C in 900 mL of hydrochloric acid (HCl) pH 1.4 containing sodium lauryl sulfate (SLS) 0.1% (w/v), at a rotation speed of 50 rpm. The dissolution behavior of carvedilol structures was studied in a dissolution tester Distek Evolution 6100. Aliquots of 10 mL were withdrawn at specific time interval and analyzed immediately in a Shimadzu UV-1800 spectrophotometer at wavelength of 285 nm. Concentrations were calculated using a calibration curve. Three replicate analyses were performed for each sample. The powder dissolution test was undertaken using 25 mg of carvedilol. For intrinsic dissolution tests, 120 mg of carvedilol was placed in the 0.8 cm diameter die cavity. The punch, die and press plate were placed in a laboratory press and kept under 1600 psi per 1 minute. The press plate was disconnected from the die to expose a compact pellet of 0.5 cm² surface area. The systems were then submitted to the test. Intrinsic dissolution rates (IDRs) were calculated by a linear regression analysis of the amount of carvedilol dissolved per unit surface area of the compressed disk, over 30 min. The discs were characterized by DSC, before and after the dissolution test, to exclude phase transitions during compression and during the

dissolution experiment. Equilibrium solubility was determined into the same medium used in the dissolution test to ensure that sink condition was maintained. Excess of powdered sample was added to 5 mL of medium, and the resulting suspension was stirred at room temperature for 24 h. The suspension was filtered and concentrations were determined by a Shimadzu UV-1800 spectrophotometer based on the absorbance at 285 nm.

Theoretical Calculations

The evaluation of the classic and non classic hydrogen bonds between the molecules in carvedilol structures was carried out with quantum chemistry program package Gaussian 09W²⁹, using the WB97XD functional³⁰ with the 6-311+G(d,p) basis set.³¹ This functional uses a version of Grimme's D2 dispersion model.³² The energy involved in the intermolecular interactions present the crystal packing were calculated using molecular dimers and trimers. Thus, the single point calculations were carried out to determine the energies of intermolecular interactions between the molecular aggregates. This energy was calculated using the equation $E_{\text{dimer}} = E(\text{PV}) - E(\text{P}) - E(\text{V})$ or $E_{\text{trimer}} = E(\text{PVU}) - E(\text{P}) - E(\text{V}) - E(\text{U})$, where the dimer $E(\text{PV})$ and $E(\text{VU})$ or trimer $E(\text{PVU})$ represents the energy of the supermolecule and $E(\text{P})$, $E(\text{V})$, $E(\text{U})$ are the energies of the monomers. The calculations were performed without symmetry constraint for molecular aggregates chosen. The partial atomic charge and the electrostatic potential (ESP) of selected monomers were calculated according to the Merz-Singh-Kollman scheme.^{33,34} All the carvedilol structures and results were visualized using graphical Chemcraft program.³⁵

Results and Discussion

Material Characterization

X-Ray Diffraction

The PXRD patterns of the samples showed sharp diffraction peaks, indicating their crystalline nature. Three unique PXRD patterns were observed, as shown in Fig. 2. The experimental powder patterns of the raw material and crystals obtained from hot toluene solution are consistent with the pattern simulated from the crystal structure II²² (Fig. 2).

The experimental PXRD pattern of the carvedilol crystals obtained by evaporation from ethyl acetate solution did not match to the calculated ones from single-crystal X-ray diffraction data of polymorphs I and II described in the literature.²¹⁻²² At the end of the research the crystalline structure of the hemihydrate was solved and published in the literature²³, allowing comparison between the powder patterns. Thus, as shown in Fig. 2, the experimental pattern of the sample obtained from ethyl acetate solution was consistent with the diagram simulated from the hydrate.²³

Because the experimental pattern of the sample obtained by crystallization from methanol did not match to the simulated patterns calculated from single-crystal data of polymorphs I²¹, II²² and of the hydrate form²³, it could be concluded that a different solid form was obtained (named III).

Carvedilol form I, polymorph already reported^{13,21} was not obtained despite significant effort. Experimental methods to prepare this crystal form are not well described. Carvedilol polymorph I was reported in one patent¹³ and the same conditions

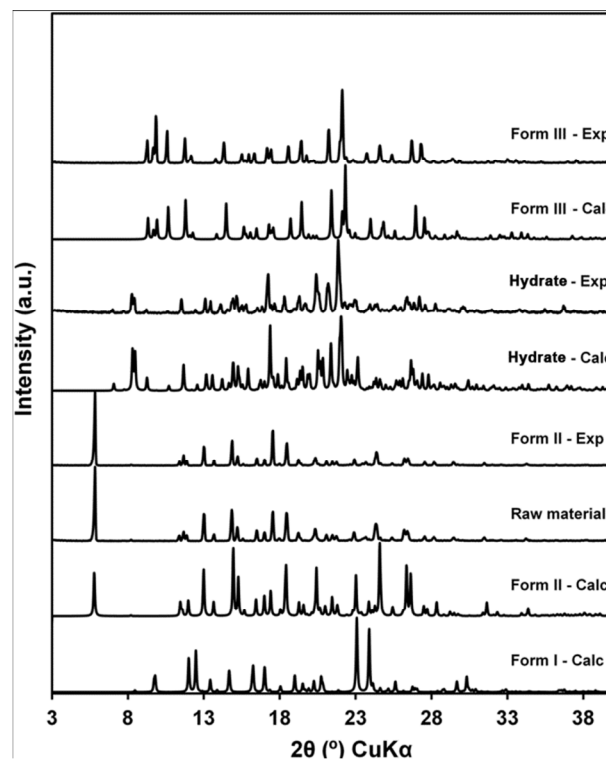


Fig. 2. PXRD patterns of carvedilol in I calculated, II calculated, raw material, II crystallized form hot toluene solution, hydrate calculated, hydrate crystallized form ethyl acetate, III calculated and III crystallized from methanol.

were tested; nevertheless, form I was not crystallized in this study.

Carvedilol structures of the hydrate form and of polymorph III were obtained from ethyl acetate and methanol, respectively, as crystals of suitable size. Thus, their crystal structures were determined by single-crystal X-ray diffraction studies. The crystal data of the hydrate and polymorph III is summarized in Table 1, together with polymorphs I and II. The hydrate and form III crystallize in the monoclinic system $P2_1/n$. When performing the experiment at low temperature, it was possible to describe the positional disorder in the aliphatic chain of the two independent carvedilol molecules in the hydrate (molecules A and B). The disorder in the N2 atom of molecule B and its consequences that affects the crystal packing and properties of this crystalline form was not reported in the original article²³ (discussed throughout the text).

The high crystallographic purity of polymorphs II and III and of the hydrate could be confirmed by comparing the experimental powder patterns to those calculated from single-crystal X-ray diffraction data. The slight differences observed by both patterns can be attributed to preferred orientation and thermal contraction (Fig. 2).

Crystal Habit Analysis

Crystal morphology plays a valuable role in the quality and efficacy of solid dosage forms.³⁶ Differences in crystal habit can remarkably change properties of a drug powder, as flowability, packing, compaction, compressibility and dissolution.³⁷ The

Cite this: DOI: 10.1039/c0xx00000x

www.rsc.org/xxxxxx

ARTICLE TYPE

Table 1 Crystal Data and Summary of the Data Collection and Structure Refinement for Carvedilol Polymorphs I, II and III and Hydrate Form.

	I ^a	II ^b	III	Hydrate
Empirical Formula	C ₂₄ H ₂₆ N ₂ O ₄	C ₂₄ H ₂₆ N ₂ O ₄	C ₂₄ H ₂₆ N ₂ O ₄	C ₂₄ H ₂₆ N ₂ O ₄ ·0.5H ₂ O
Formula Weight	406.47	406.47	406.47	415.48
Temperature(K)	295	173	150	150
Crystal System	Monoclinic	Monoclinic	Monoclinic	Monoclinic
Space Group	P2 ₁ /c	P2 ₁ /c	P2 ₁ /n	P2 ₁ /n
<i>a</i> (Å)	9.094(1)	15.5414(14)	11.2908(3)	13.4774(3)
<i>b</i> (Å)	12.754(1)	15.2050(12)	12.2293(3)	16.5146(3)
<i>c</i> (Å)	18.330(2)	9.1174(8)	14.9933(4)	19.1385(4)
α (°)	90	90	90	90
β (°)	97.36(1)	100.730(7)	91.389(3)	94.160(3)
γ (°)	90	90	90	90
Volume (Å ³)	2108.49(9)	2116.83(3)	2069.65(9)	4248.5(15)
<i>Z</i>	4	4	4	4
<i>d</i> _{calc} (Mg/m ³)	1.280	1.275	1.304	1.299
μ (mm ⁻¹)	- ^c	0.09	0.09	0.09
Reflns. collected	-	12521	22151	77946
Unique reflns.	-	3956	3656	7775
Observed reflns.	-	3060	3122	6357
R (int)	-	0.034	0.039	0.034
Restraints	-	0	0	14
Parameters	-	285	273	592
<i>R</i> ₁	0.037	0.040	0.042	0.040
<i>wR</i> ₂	-	0.106	0.109	0.107
GOOF on F ²	-	1.03	1.05	1.05

^a Data for structure I are in the literature ²¹. ^b Data for structure II are in the literature ²². ^c Unavailable information in CSD.

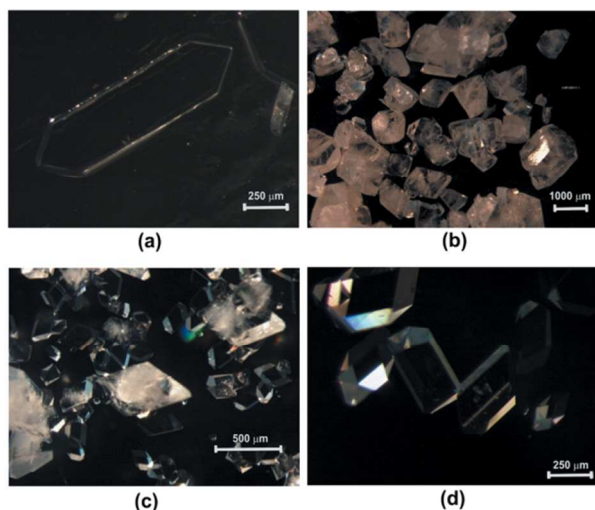


Fig 3 Optical microscope images of carvedilol in (a) II at 63x magnification, (b) hydrate at 10x magnification, (c) III at 40x magnification and (d) III at 63x magnification.

morphological features of polymorphs II and III and of the hydrate form were visually examined using optical microscopy and are displayed in Fig. 3. Carvedilol structure II crystallized from hot toluene solution occurs as plates. Changes in crystal habit were observed in the hydrate form, crystallized from ethyl acetate solution (tabular). Carvedilol polymorph III, obtained

from methanol solution, showed morphology similar to the hydrate form.

Thermal Analysis

Thermal methods can be used to clearly distinguish between polymorphs and solvates by the event of desolvation in the latter.³⁸ Fig. 4 shows DSC and TGA profiles of carvedilol structures II, hydrate and III. The DSC curve of polymorph II shows one sharp endothermic peak at 119 °C ($T_{\text{onset}} = 115$ °C; $\Delta H = 116.6$ J/g). Carvedilol polymorph III exhibit a similar DSC profile but with a higher endothermic peak, at 126 °C ($T_{\text{onset}} = 124$ °C; $\Delta H = 123.8$ J/g). In addition, no mass loss was observed in either TGA profiles, when both polymorphs were heated up to 150 °C, confirming that the DSC peaks were related to melting and indicating their anhydrous nature. The results obtained by DSC seemed to suggest a weaker intermolecular linkage in structure II than in III, confirmed by the comparative structure study.

The DSC curve of the hydrate form shows one endothermic peak at 107 °C ($T_{\text{onset}} = 98$ °C; $\Delta H = 115.2$ J/g). The TGA profile showed mass loss of 2.2%, associated to one water molecule per two carvedilol molecules in the crystal structure of the hydrate form, as concluded in the crystallographic study. Karl Fischer analysis was used as a complementary technique. The result indicated a water content of 2.2% in carvedilol crystals obtained from ethyl acetate solution.

The DSC broad endotherm of the hydrate corresponds to the weight loss observed by TGA and to the melting of the structure.

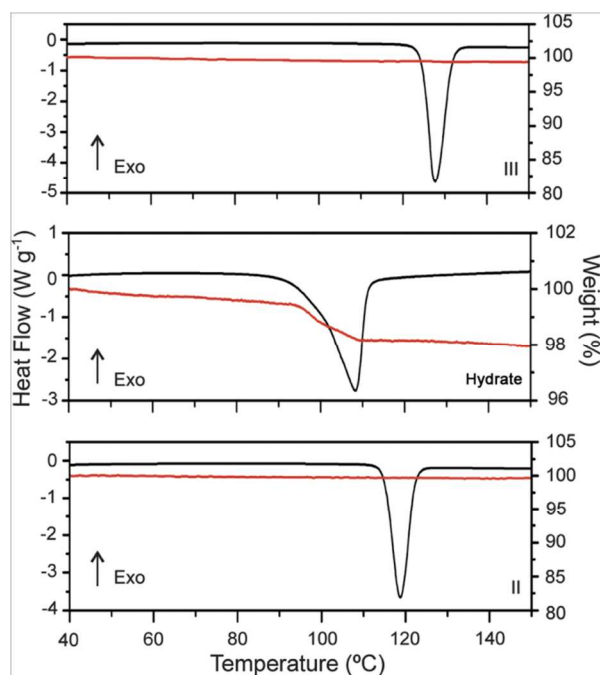


Fig. 4 DSC (black) and TGA (red) curves of carvedilol in II, hydrate and III at 10 °C min⁻¹ heating rate.

However, we can not use this endotherm as a thermodynamic characteristic of the hydrate³⁹ because the thermal events resulted in a complex signal in the DSC curve, being this signal dependent on the measurements conditions. During the heating, the API may have partially dissolved in the water of crystallization. This can be the reason why the melting peak of the hydrate was much broader than the melting peaks of II and III. But even if it did not happen, the melting of the crystal and dissolution of the melt may have taken place at the same time resulting in a broad signal in the DSC curve.

15 Structural Analysis

Carvedilol polymorphs I²¹, II²² and III crystallize in the centrosymmetric monoclinic space group with four molecules (comprising two pairs of enantiomeric molecules) per unit cell. The hydrate contains two independent carvedilol molecules (molecules A and B) and one water molecule in the asymmetric unit. Although the crystallization experiment was carried out in ethyl acetate, traces of water present in the solvent or the

Table 2 Selected Torsion Angles (°) for Carvedilol in I, II, and III and Hydrate Form. Major Site for Disordered Atoms was Selected for Molecules A and B of the Hydrate.

Torsion Angles	I ^a	II ^b	Hydrate Molecule A	Hydrate Molecule B	III
C12-C1-O1-C13	175.2(2)	-164.1(1)	171.1(1)	-175.1(2)	177.3(3)
C1-O1-C13-C14	-177.2(2)	173.5(1)	100.1(2)	163.7(4)	-175.5(1)
O1-C13-C14-C15	-59.2(2)	-170.4(1)	164.1(2)	-56.3(6)	61.5(2)
O1-C13-C14-O2	-179.5(2)	69.0(1)	-74.5(3)	176.3(4)	-62.3(2)
O2-C14-C15-N2	-56.8(2)	-54.8(1)	65.8(3)	-62.1(7)	-66.2(2)
C13-C14-C15-N2	-175.0(2)	-178.2(1)	-170.0(2)	176.1(4)	169.3(3)
C14-C15-N2-C16	-167.3(2)	174.4(1)	-173.3(2)	168.9(5)	-175.2(1)
C15-N2-C16-C17	-177.8(2)	-169.9(1)	178.6(2)	-172.4(4)	-178.4(1)
N2-C16-C17-O3	64.1(2)	63.7(2)	63.5(2)	65.8(2)	-61.1(2)
C16-C17-O3-C18	-159.8(2)	-161.7(1)	-177.1(1)	172.8(1)	-176.0(1)
C17-O3-C18-C19	-30.2(3)	-54.2(2)	4.9(2)	-6.6(2)	-5.8(2)

^a Data for structure I are in the literature^{21,22}. ^b Data for structure II are in the literature²².

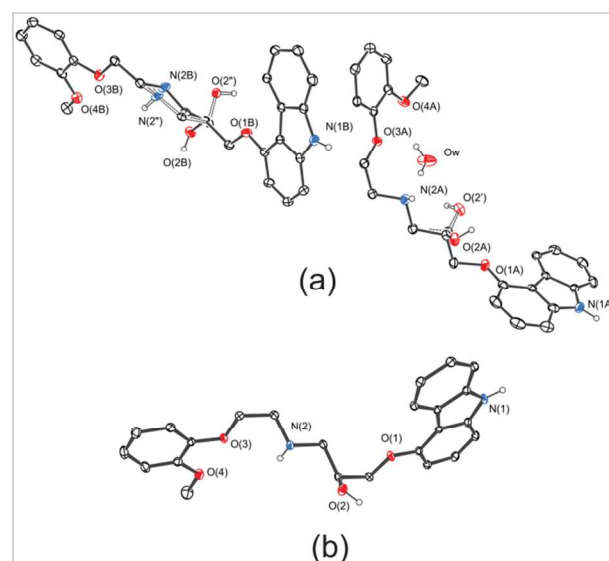


Fig. 5 ORTEP drawing of carvedilol in (a) hydrate and (b) polymorph III. Thermal ellipsoids are drawn at the 50% probability levels.

humidity of the environment may have led to the formation of a hydrate form.

In carvedilol molecules A and B of the hydrate, the C14 e O2 atoms displays positional disorder; these atoms are statistically distributed over two sites. Even more, in molecule B, positional disorder occurs for the N2 and C15 atoms. The aliphatic central chain was split into two positions, with site-occupation factors of 0.764(3):0.236(3) for molecule A and 0.704(3):0.296(3) for molecule B. Molecules A and B of the hydrate are shown in Fig. 5a and in Fig. 6.

The ORTEP drawing in Fig. 5a clearly shows the positional disorder in molecules A and B of the hydrate. Moreover, Fig. 5 illustrates the conformational changes in carvedilol hydrate and polymorph III, mainly related to different orientations of the carbazol-4-yloxy moiety. Different orientations of the methoxyphenoxy moiety are also observed. The conformational differences can be better visualized in Fig. 6, which shows the S-enantiomers of carvedilol in I, II, hydrate and III superimposed in a capped stick fashion. A typical case of conformational polymorphism is described for carvedilol based on this study.

When comparing the torsion angles that describe the conformation of the aliphatic central chain, one can see that in all crystal structures the angles C13-C14-C15-N2, C14-C15-N2-C16

Cite this: DOI: 10.1039/c0xx00000x

www.rsc.org/xxxxxx

ARTICLE TYPE

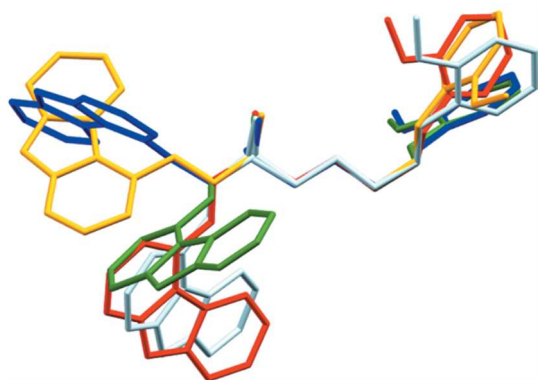


Fig. 6 Superposition of the carvedilol S-enantiomers in I (red), II (yellow), III (green), hydrate molecule A (blue) and molecule B (light blue). Hydrogen atoms were hidden for clarity.

5 and C15-N2-C16-C17 are geometrically similar. The aliphatic central chain involving the C13-C14-C15-N2-C16-C17 atoms adopts a rather planar conformation, differing by a few degrees from 180° (Table 2).

Table 2 shows differences in the torsion angle O1-C13-C14-C15 between carvedilol crystalline structures. Higher values are observed in molecule A of the hydrate and in II, with the O1-C13-C14-C15 atoms in the anti-conformation. This torsion angle is responsible for the orientation of carbazol-4-yloxy moiety that, in these molecules is on the same side of the methoxyphenoxy moiety, with respect to the horizontal plane formed by the aliphatic central chain, as shown in Fig. 6.

In Fig. 6, it also is possible to observe differences in the orientation of the carbazol-4-yloxy moiety with regard to hydroxyl moiety. The hydroxyl group has similar orientations in

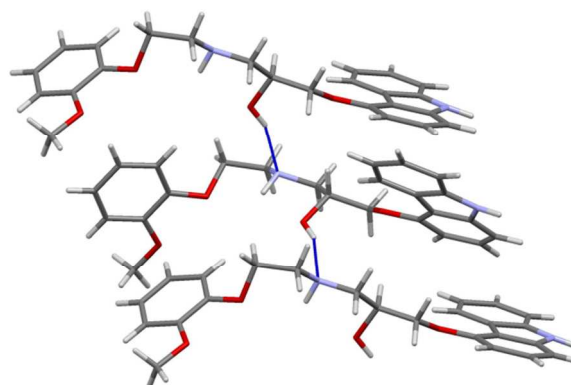


Fig 7 Hydrogen bonds connecting molecules of carvedilol in structure II in a C5 motif.

all crystalline structures, as evidenced by the torsion angle O2-C14-C15-N2 in a gauche-conformation. The different orientation of the carbazol-4-yloxy moiety results in different values of the torsion angle O1-C13-C14-O2. These atoms adopt an anti-conformation in in molecule B of the hydrate. The hydroxyl and the carbazol-4-yloxy moieties are more close together in the structures II and III and in molecule A of the hydrate (Table 2 and Fig.6).

The inspection of the crystal packing revealed that the hydrogen bond patterns are different for each structure (Table 3). Their crystal assemblies are strongly dependent on the molecular conformations. The crystal structure analysis of carvedilol in II showed two classic hydrogen bonds (Fig 7): the interaction N1-H1...O4 forms a C(16) chain extending along the crystallographic b axis, and the intermolecular hydrogen bond O2-H2O...N2 forms a chain with C(5) graph set motif in [0 0 1]

Table 3 Hydrogen Bonding Network (Å, °) for Carvedilol Polymorphs II and III and Hydrate Form.

Structure		D-H...A ^a	H...A	D...A	D-H...A	Symmetry Code
II ^b		O2-H2O...N2	2.09	2.963(2)	158	$x, 1/2-y, 1/2+z$
		N1-H1...O4	2.11	3.034(2)	168	$1-x, 1/2+y, 3/2-z$
		N1-H1...O3	2.47	3.085(2)	123	$1-x, 1/2+y, 3/2-z$
Hydrate ^c	Major occupancy	OW-HW1...O4A	2.10	2.895(2)	160	
		OW-HW1...O3A	2.43	2.974(2)	124	
		OW-HW2...N2A	1.95	2.785(2)	174	
		N1A-H1A...OW	2.04	2.817(2)	147	$3/2-x, -1/2+y, -1/2-z$
		O2B-H2BO...OW	2.34	3.210(6)	163	$-1/2+x, 3/2-y, 1/2+z$
		N2B-H2BN...O2B	2.19	2.826(5)	125	$1-x, 2-y, 1-z$
	Minor occupancy	N1B-H1B...CgB ^d	2.37	3.194	161	$1/2+x, 3/2-y, 1/2+z$
		O2A-H2AO...N2B	2.01	2.835(4)	167	$3/2-x, -1/2+y, -1/2-z$
		O2B-H2BO...O2'	2.19	2.763(4)	124	$-1/2+x, 3/2-y, 1/2+z$
		O2''-H2''O...O3B	2.48	3.053(6)	127	$1-x, 2-y, 1-z$
		O2''-H2''O...O4B	1.89	2.702(4)	162	$-1-x, 2-y, 1-z+z$
		N2B-H2BN...O2B	2.18	2.826(6)	124	$1-x, 2-y, 1-z$
		O2'-H2'O...OW	2.26	2.641(6)	108	
III	N2-H2N...O2	2.68	3.503(2)	159	$-x, -y, -z$	
	O2-H2O...O4	2.02	2.834(2)	164	$-x, -y, -z$	
	N1-H1...O2	2.04	2.883(2)	160	$1/2+x, -1/2-y, -1/2+z$	

^a D, hydrogen donor; A, hydrogen acceptor. ^b Data for structure II are in the literature ²². ^c Minor occupancy disorder atoms are represented with ' in molecule A and with '' in molecule B. ^d Relative to 2-methoxyphenoxy ring.

Cite this: DOI: 10.1039/c0xx00000x

www.rsc.org/xxxxxx

ARTICLE TYPE

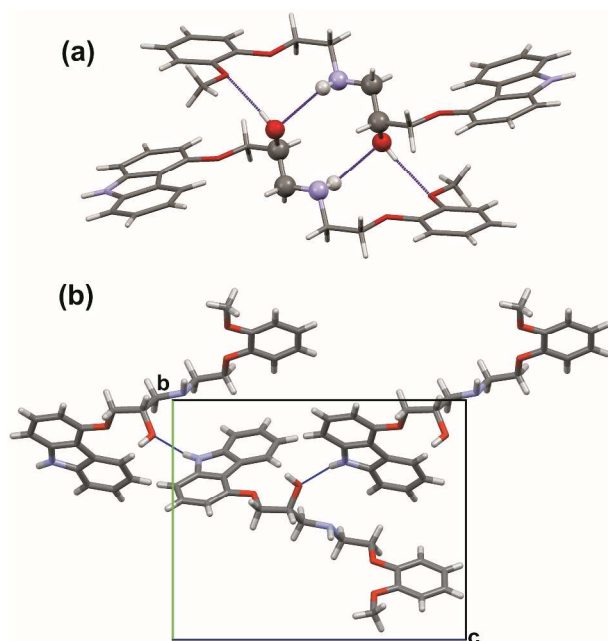


Fig. 8 Hydrogen bonds in carvedilol structure III. (a) $R_2^2(10)$ hydrogen bond ring motif are shown in ball and stick model and (b) C9 hydrogen bond chain motif.

direction.⁴⁰

The main intermolecular interactions responsible for maintaining the arrangement of the crystalline structure III are three classic hydrogen bonds. The main details of their geometry are given in Table 3. Fig. 8 shows the hydrogen bonding pattern of the structure III. The interactions $O2-H2O\cdots O4$ and $N2-H2N\cdots O2$ result in the formation of a dimer with the $R_2^2(22)R_2^2(10)$ hydrogen bond ring motif (Fig. 8a). One dimer is linked to another one along the $[0 -1 0]$ and $[1 0 -1]$ directions, via $N1-H1\cdots O2$ hydrogen bonds that connect two adjacent molecules in a zigzag motif with $C_2^2(14)$ and C(9) chains, respectively (Table 3 and Fig. 8b).

The presence of water molecules leads to formation of a complex multi-dimensional hydrogen-bonded and supramolecular networks in the hemihydrate, as we can see in Fig. 9. The occupational disorder is responsible to the complexity of the interaction pattern in this crystal. The higher levels of graph set consist of multiple ring and chain motifs.

Analyzing the molecules A with major occupancy atoms, a chain motif along the $[0 1 0]$ and $[1 0 1]$ directions is formed. In this case, the interactions between the molecule A and the water molecule results in a zigzag chain $C_2^2(12)$ along the crystallographic b axis (Table 3 and Fig. 9a). With respect to molecule B, the interaction $N2B-H2BN\cdots O2B$ leads to the formation of a dimer with the a $R_2^2(10)$ ring as the basic graph unitary set (Fig. 9b). These dimeric systems of molecules B bind to the chain formed by molecules A and water molecules, through

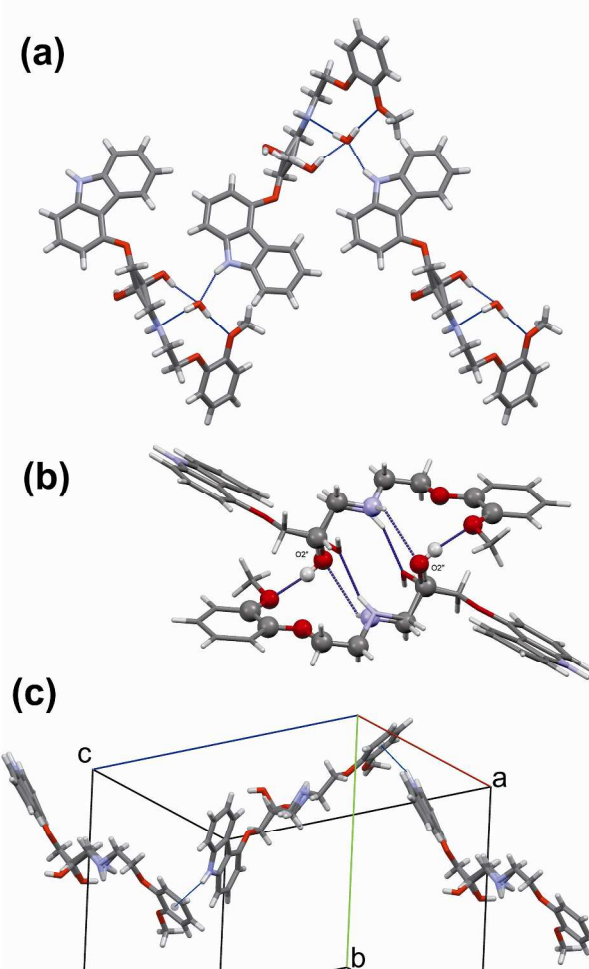


Fig. 9 Hydrogen bonds in carvedilol hydrate: (a) chain $C_2^2(12)$ between molecules A and water molecules (b) ring graph set motif with $R_2^2(22)$ are shown in ball and stick model and (c) chain of molecules B.

the interaction $O2A-H2A\cdots N2B$, resulting in an infinite chain along the $[1 0 1]$ direction.

The molecule B, with minor occupancy atoms, presents the interactions $N2''-H2''N\cdots O2''B$ and $O2''B-H2''O\cdots O4B$ (Table 3) that forms a dimer with multiples rings with graph set $R_2^2(22)[R_2^2(10)]$, similar to the one observed in carvedilol structure III. The disorder in molecule A leads to the formation of one additional weak hydrogen bond $O2B-H2BO\cdots O2'$, which also connects the molecules B with the chain of the molecules A (Table 3). Thus, the $N2''$ atom in the amino group of the disordered molecule B, does not act as a hydrogen bond acceptor. The intermolecular interaction $O2-H2O\cdots N2$ is responsible for the change in the dissolution of carvedilol structures (discussed below). This hydrogen bond occurs in polymorph II and in the hydrate form. In the hemihydrate, connects disorder parts of molecules A and B (Table 3). However, in structure III, the

torsion angles O1-C13-C14-C15 and O1-C13-C14-O2, both in the gauche conformation, prevent the formation of the intramolecular interaction O2—H2O···N2 in this polymorph. Thus, in form III the nitrogen atom of the aliphatic central chain (N2) does not act as a hydrogen bond acceptor and in molecule B of the hydrate this atom is a partial acceptor.

Powder and Intrinsic Dissolution Tests

Solid forms of an API can exhibit differences in solubility, dissolution rate and bioavailability. The powder dissolution behaviors of the individual structures determined in HCl pH 1.4 containing SLS 0.1% (w/v) are demonstrated in Fig. 10a. Carvedilol structure III exhibited rapid dissolution, reaching 85 % of the dose in less than 30 minutes. The other crystal structures did not dissolved above 85 % of the dose; the hydrate showed the slowest dissolution during the whole test. During the tests, it was assumed that sink conditions were maintained because concentrations were below 5% of the saturation solubility (0.92 mg/mL for structure III).

An important factor determining the dissolution rate in powder methods is the particle size of the API. The dissolution rate increases with decreasing particle size. Therefore, to eliminate the influence of the particle size and agglomeration and enable further characterization of the crystal forms with respect to their dissolution profiles, intrinsic dissolution tests were carried out. Intrinsic dissolution profiles of carvedilol structures in HCl pH 1.4 containing SLS 0.1% (w/v) are shown in Fig. 10b. The results showed good linearity between time and concentration. Intrinsic dissolution rates of II, hydrate and III, which were calculated from the slope of each plot (Fig. 10b) were 223, 331 and 349 $\mu\text{g}/\text{cm}^2/\text{min}$, respectively. Carvedilol polymorph III showed higher IDR than II, but carvedilol hydrate and polymorph III did not show IDRs statistically different from each other.

Usually, the most stable solid form has the slowest dissolution rate.¹ However, the highest dissolution rate of carvedilol structure III (stable polymorph compared to polymorph II, observed by DSC) suggests that other features influenced the dissolution test. Carvedilol is a base compound that contains an α -hydroxyl secondary amine, with a pK_a of 7.6. Carvedilol exhibits pH dependent solubility. In alkaline medium, with pH above 9, carvedilol solubility is relatively low. Its solubility increases as pH decreases, due to protonation.⁴¹ It has already been demonstrated that protonation occurs in the secondary amine of the aliphatic central chain; the amine from carbazole moiety remain unchanged.⁴² Thus, it becomes clear that in the dissolution medium used (pH 1.4), carvedilol molecules undergo protonation in the secondary amine. This feature influenced the dissolution test of carvedilol structures. As shown in the crystallographic study, the crystal structure II exhibits an O2—H2O···N2 hydrogen bond, which is not present in the structure III. The nitrogen atom of the secondary amine in III does not participate in hydrogen bonds as hydrogen acceptor, thus making the pair of electrons on the nitrogen more available to receive a proton. This structural feature enabled us to suggest that in the dissolution test, in an acid medium, carvedilol in III has higher protonating ability, which led to higher IDR, although its greater stability observed by DSC.

Studies were already conducted to explain the lack in correlation

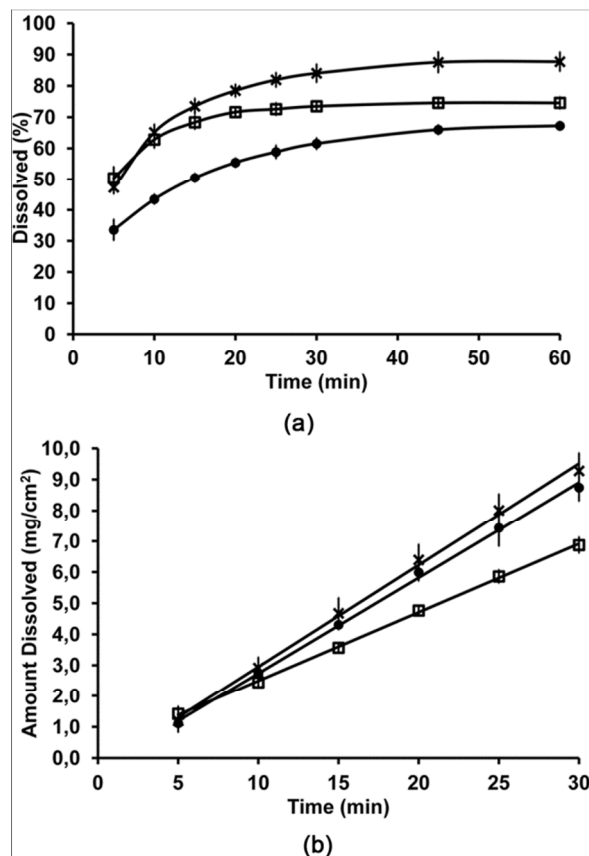


Fig. 10 Dissolution profiles of carvedilol in II (□), hydrate (●) and III (x), (n = 3, mean \pm S.D.). (a) Powder dissolution and (b) intrinsic dissolution.

between structure features and physicochemical properties. As an example, indomethacin polymorphs have no correlation between packing density and reactivity. Although indomethacin α -form has higher density than γ -form, the α -form reacts with ammonia vapor while the γ -form is inert. The crystal packing leads to easy accessibility of the carboxylic acid groups in the α -form, and this, combined with the weak hydrogen bond of the carboxylic acid group, leads to higher reactivity of α -form.⁴³

The carvedilol hydrate form also showed higher dissolution rate than polymorph II (Fig. 10b). The hydrogen bond O2—H2O···N2 is also present in the hydrate, but the nitrogen atom N2 is partially available to protonation; this could be the reason why this hydrate have higher dissolution rate under the experimental conditions used.

Because it is a poorly water soluble API, many methods are proposed to improve the dissolution and solubility of carvedilol.^{41,44,45} Salt formation is one of these methods.⁴⁶ However, without changing the composition, the use of polymorph III, with higher melting point and higher dissolution than polymorph II, can be an interesting strategy for carvedilol development. But it is also important to study mechanical properties of carvedilol polymorphs, study not yet performed.

Theoretical Calculations

The aggregates of the molecules analyzed through theoretical studies are presented in Fig. 11, which also shows the chosen molecular units (P, V e U). Carvedilol structures (II, hydrate-A,

Cite this: DOI: 10.1039/c0xx00000x

www.rsc.org/xxxxxx

ARTICLE TYPE

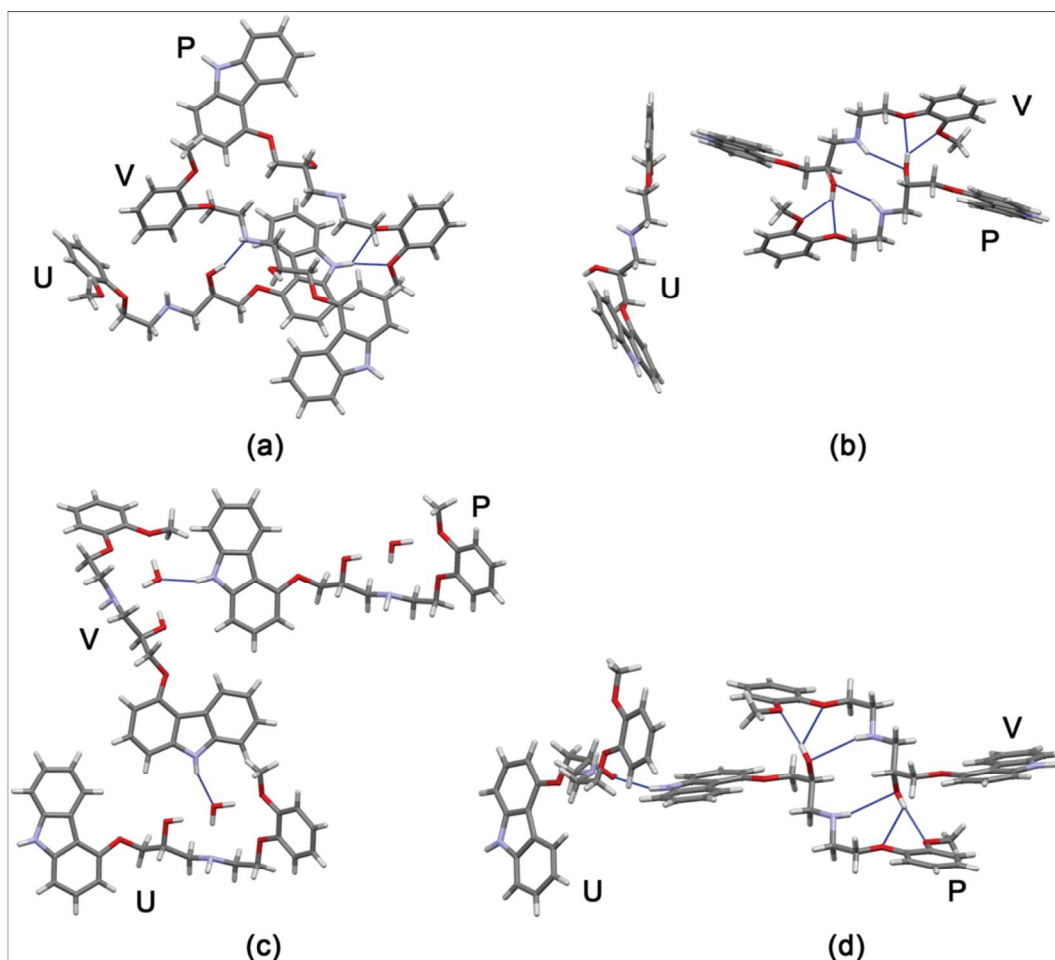


Fig. 11 Aggregates evaluated by the interaction of the molecular units (P, V e U) in carvedilol (a) II, (b) hydrate-B, (c) hydrate-A and (d) III.

hydrate-B and III) were calculated as trimers (PVU) and dimers (PV and VU). The interaction energies are presented in Table 4. Some intermolecular distances obtained by crystallographic analysis in Table 2 are also shown in Fig. 11. These interactions allowed the selection of these aggregates according to the crystalline packings of each structure. For example, structure II has crossed interaction between molecules PU and VU, while the other structures are characterized by aggregates with an organization PV and VU, which forms well defined chains. Even the hydrate, which was subdivided into anhydrous chain (B) and hydrated (A), shows this organization. The values of interaction energy between molecules in these aggregates explain some experimental observations originated by the crystal packing.

Analyzing the interaction energy in the trimer, we found greater stabilization for the structure II, -49.71 kcal/mol, followed by structures III and hydrate-B, -46.20 and -39.46 kcal/mol, and finally by hydrate-A which is less stabilized with -24.98 kcal/mol. In this case, the water molecule in the hydrate establishes a molecular distortion which increases the steric

hindrance of carvedilol, reducing the number of classic hydrogen bonds between the molecules in the aggregates. These observations are corroborated by the DSC results previously discussed. The melting points were higher for anhydrous polymorphs than for hydrated form. The water molecules destabilize the hydrate form by reducing the number of intermolecular interactions. These observations are best understood when we analyze the interactions in the PV dimers in Table 4. For example, these dimers are more stabilized in the polymorph III and hydrate-B with -36.61 and -30.60 kcal/mol, respectively. On the other hand, this dimer in the structure II is

Table 4 Intermolecular Interaction Energy (kcal/mol) Analysis for PVU Trimer and PV and VU Dimers.

Aggregates	Trimer (PVU)	Dimer (PV)	Dimer (VU)
Polymorph II	-49,71	-26,65	-18,03
Hydrate-A	-24,98	-12,30	-12,30
Hydrate-B	-39,46	-30,60	-8,66
Polymorph III	-46,20	-36,61	-9,22

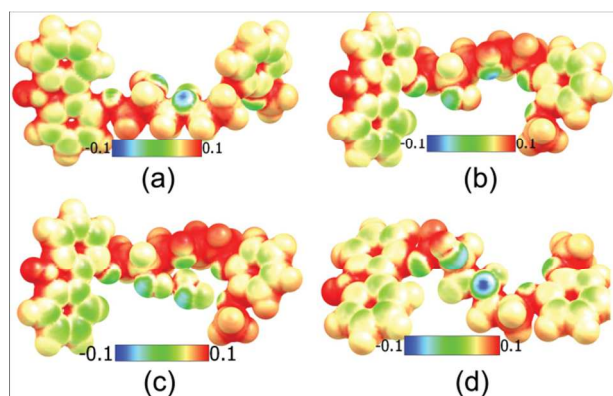
Cite this: DOI: 10.1039/c0xx00000x

www.rsc.org/xxxxxx

ARTICLE TYPE

Table 5 Atomic Charge Selected According to Merz-Singh-Kollman Scheme.

Aggregates	O4	O3	O2	H2O	O1	N2	H2N	N1	H1
Polymorph II	-0.384	-0.342	-0.714	0.435	-0.407	-0.789	0.453	-0.648	0.400
Hydrate-A	-0.224	-0.337	-0.610	0.367	-0.285	-0.236	0.223	-0.770	0.455
Hydrate-B	-0.419	-0.389	-0.785	0.489	-0.358	-0.570	0.347	-0.746	0.448
Polymorph III	-0.370	-0.425	-0.797	0.509	-0.330	-0.674	0.322	-0.693	0.434

**Fig. 12** Electrostatic potential surfaces of carvedilol in (a) II, (b) hydrate-B, (c) hydrate-A and (d) III.

stabilized with -26.65 kcal/mol and is much less stabilized in hydrate-A, -12.30 kcal/mol. If we consider an average between hydrate-A and hydrate-B, we have a value of -21.45 kcal/mol, lower than other structures. However, for the VU dimer, we found a decrease in stabilization as a result of the smaller number of intermolecular interactions, with the structure II being favoured by -18.03 kcal/mol. This represents an inversion in the tendency of stabilization observed in PV dimer. These calculated values show a strong dependence of the stereo effect and electrostatic character of the groups that establish hydrogen bonds.

The atomic charges obtained by population analysis according to the Merz-Singh-Kollman scheme were also evaluated (Table 5). The oxygen and nitrogen atoms were selected because they are the most electronegative elements and can form strong intermolecular interaction. In carvedilol molecule (Fig. 1), the aliphatic chain has two atoms with high negative charge, the oxygen (O2) of the hydroxyl group and nitrogen (N2) of the imino group. This molecule also has other nitrogen (N1) with a high negative charge in carbazol-4-yloxy group. These atoms are bonded with hydrogen atoms with high positive charge. This indicates an electronic deficiency that justifies the formation of hydrogen bonds. However, evaluating the data for hydrate-A, a significant reduction in the charges of O2 and N2 atoms in the aliphatic chain was observed. This shows that the water molecule reduces the possibilities of interactions between carvedilol molecules in this position, which explains the destabilization. However, N1-H1 in carbazol-4-yloxy group allows the formation of hydrogen bonds that stabilize the structures.

Electrostatic potential surfaces (ESP) of the anhydrous and

hydrated molecules are shown in Fig. 12. These surfaces permit an interpretation of the overall charge distribution of the molecules. Red color describes the concentration of positive charge and blue color describes the concentration of negative charge. For anhydrous molecules, the imine nitrogen of the aliphatic chain is the most negatively charged element. In the opposite way, the nitrogen in carbazol-4-yloxy group is more positively charged. Fig. 12 shows possible sites for electrostatic interaction and the influence of the steric hindrance caused by the water molecule and the twisting of the carbazol-4-yloxy and 2-methoxyphenoxy groups, especially in the hydrate-B. In terms of electrostatic, the benzenoids groups have a neutral characteristic even in the presence of more electronegative atoms.

Conclusions

The crystal structure of one anhydrous form was elucidated for the first time and the hemihydrate of carvedilol was redetermined. Both structures were compared to the previously reported polymorphs I and II. All structures crystallize in the centrosymmetric monoclinic space group. The solid forms II, hydrate and III can be distinguished by thermal analysis and crystallographic methods because of differences in their melting points and unique PXRD peaks. Carvedilol is an example of conformational polymorphism. Carvedilol crystal forms are characterized by variations in intermolecular and intramolecular hydrogen bonds. The polymorphs II and III and the hydrate exhibit different dissolution profiles in acid medium. The intrinsic dissolution test revealed that carvedilol in III has higher IDR than in II in acid medium, despite its greater stability. The hydrogen bond pattern can explain this phenomenon. The theoretical results corroborate these observations evaluated, emphasizing the importance of intermolecular interaction obtained by classic and non-classical hydrogen bonds. This work emphasizes the importance of the structural analysis and shows that there is a potential strategy for carvedilol development.

Acknowledgment

The authors thank LabCri (UFMG) and LdrX-UFF for X-ray facilities and CNPq for financial support.

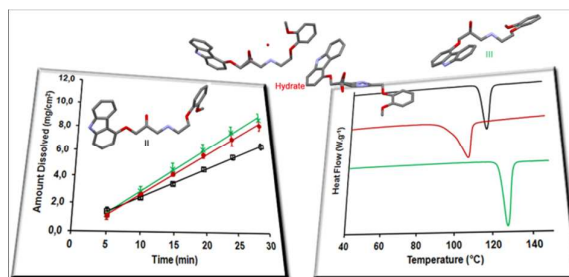
Notes and references

^a Instituto de Química, Universidade Federal Fluminense, Outeiro de São João Batista s/n°, Niterói, 24020-150, RJ, Brazil. Fax: +5521 2629 1229; Tel: +5521 2629 2128; E-mail: liviaderis@gmail.com

^b Laboratório de Sistemas Farmacêuticos Avançados, Complexo Tecnológico de Medicamentos – Farmanguinhos, Fundação Oswaldo

- Cruz, Avenida Comandante Guarany, 447, Rio de Janeiro, 22775-903, RJ, Brazil Fax: +5521 3348 5050; Tel: +5521 3348 5319
- † Electronic Supplementary Information (ESI) available: CCDC reference number 901309 (hydrate) e 901308 (polymorph III). For ESI and crystallographic data in CIF or other electronic format see DOI: 10.1039/b000000x/
1. D. J. W. Grant, in *Polymorphism in Pharmaceutical Solids*, ed. H. G. Brittain, Marcel Dekker, New York, 1999, pp 1-33.
 2. G. R. Desiraju, *Cryst. Growth Des.*, 2008, **8**, 3-5.
 3. J. Bernstein, R. J. Davey, J. O. Henck, *Angew. Chem. Int. Ed. Engl.*, 1999, **38**, 3441-3461.
 4. L. F. Huang, W. Q. Tong, *Adv. Drug Delivery Rev.* 2004, **56**, 321-334.
 5. G. P. Stahly, *Cryst. Growth Des.*, 2007, **7**, 1007-1026
 6. M. Kitamura, *CrystEngComm*, 2009, **11**, 949-964.
 7. J. W. Chew, S. N. Black, P. S., Chow, R. B. H. Tan, K. J. Carpenter, *CrystEngComm*, 2007, **9**, 128-130.
 8. H. G. Brittain, *Polymorphism in pharmaceutical solids*, Marcel Dekker, New York, 1999.
 9. A. Pitaluga Jr, L. D. Prado, R. Seiceira, J. L. Wardell, S. M. Wardell, *Int. J. Pharm.*, 2010, **398**, 50-60.
 10. C. J. Dunn, A. P. Lea, A. J. Wagstaff, *Drugs*, 1997, **54**, 161-185.
 11. R. R. Ruffolo Jr, G. Z. Feuerstein, *Cardiovasc. Drugs Ther.*, 1997, **11**, 247-256.
 12. H. H. Zhou, A. J. Wood, *J. Clin. Pharmacol Ther.*, 1995, **57**, 518-524.
 13. *WO Pat.*, 05105, 1999.
 14. *WO Pat.*, 00216, 2002.
 15. *US Pat.*, 0152756, 2004.
 16. *WO Pat.*, 094378, 2004.
 17. *US Pat.*, 0094771, 2006.
 18. *WO Pat.*, 135757, 2006.
 19. *US Pat.*, 0148878, 2006.
 20. *US Pat.*, 7598396, 2009.
 21. W. M. Chen, L. M. Zeng, K. B. Yu, J. H. Xu, *Jiegou Huaxue*, 1998, **17**, 325-328.
 22. H. S. Yathirajan, S. Bindya, T. V. Sreevidya, B. Narayana, M. Bolte, *Acta Crystallogr. Sect. E: Struct. Rep. Online*, 2007, **E63**, o542-o544.
 23. F. Diaz, A. Benassi, M. Quintero, G. Polla, E. Freire, R. Baggio, *Acta Crystallogr Sect C: Cryst. Struct. Comm.*, 2011, **C67**, o222-o225.
 24. O. Planinšek, B. Kovačič, F. Vrečer, *Int. J. Pharm.*, 2011, **406**, 41-48.
 25. N. Sharp, *Eur. Heart J.*, 1996, **17**, 39-42.
 26. C. F. Macrae, I. J. Bruno, J. A. Chisholm, P. R. Edgington, P. McCabe, E. Pidcock, L. Rodriguez-Monge, R. Taylor, J. van de Streek, P. A. Wood. *J. Appl. Crystallogr.*, 2008, **41**, 466.
 27. G. M. Sheldrick. *Acta Crystallogr. Sect. A: Found. Crystallogr.*, 2008, **A64**, 112-122.
 28. L. J. Farrugia. *J. Appl. Crystallogr.*, 1997, **30**, 565.
 29. M. J. Frisch, G. W. Trucks, H. B. Schlegel, G. E. Scuseria, M. A. Robb, J. R. Cheeseman, G. Scalmani, V. Barone, B. Mennucci, G. A. Petersson, H. Nakatsuji, M. Caricato, X. Li, H. P. Hratchian, A. F. Izmaylov, J. Bloino, G. Zheng, J. L. Sonnenberg, M. Hada, M. Ehara, K. Toyota, R. Fukuda, J. Hasegawa, M. Ishida, T. Nakajima, Y. Honda, O. Kitao, H. Nakai, T. Vreven, J. A. Montgomery Jr. J. E. Peralta, F. Ogliaro, M. Bearpark, J. J. Heyd, E. Brothers, K. N. Kudin, V. N. Staroverov, R. Kobayashi, J. Normand, K. Raghavachari, A. Rendell, J. C. Burant, S. S. Iyengar, J. Tomasi, M. Cossi, N. Rega, J. M. Millam, M. Klene, J. E. Knox, J. B. Cross, V. Bakken, C. Adamo, J. Jaramillo, R. Gomperts, R. E. Stratmann, O. Yazyev, A. J. Austin, R. Cammi, C. Pomelli, J. W. Ochterski, R. L. Martin, K. Morokuma, V. G. Zakrzewski, G. A. Voth, P. Salvador, J. J. Dannenberg, S. Dapprich, A. D. Daniels, Ö. Farkas, J. B. Foresman, J. V. Ortiz, J. Cioslowski, D. J. Fox, *Gaussian 09, Revision A.1*, Gaussian, Inc., Wallingford, CT, 2009.
 30. J. D. Chai, M. Head-Gordon, *Phys. Chem. Chem. Phys.*, 2008, **10**, 6615-6620.
 31. V. A. Rassolov, M. A. Ratner, J. A. Pople, P. C. Redfern, L. A. Curtiss, *J. Comput. Chem.*, 2001, **22**, 976-984.
 32. S. Grimme, *WIREs Comput. Mol. Sci.*, 2011, **1**, 211-228.
 33. U. C. Singh, P. A. Kollman, *J. Comp. Chem.*, 1984, **5**, 129-145.
 34. B. H. Besler, K. M. Merz Jr., P. A. Kollman, *J. Comp. Chem.*, 1990, **11**, 431-39.
 35. G. A. Zhurko, *ChemCraft*, <http://www.chemcraftprog.com>
 36. G. Chawla, P. Gupta, R. Thilagavathi, A. K. Chakraborti, A. K. Bansal, *Eur. J. Pharm. Sci.*, 2003, **20**, 305-317.
 37. A. K. Tiwary, *Drug Dev. Ind. Pharm.*, 2001, **27**, 699-709.
 38. D. Giron. *Thermochim. Acta*, 1995, **248**, 1-59.
 39. R. Shimanovich, M. Cooke, M. L. Peterson, *J. Pharm. Sci.*, 2012, **101**, 4013-4017.
 40. J. Bernstein, R. E. Davis, L. Shimoni, N. L. Chang, *Angew. Chem. Int. Ed. Engl.*, 1995, **34**, 1555-1573.
 41. T. Loftsson, S. B. Vogensen, C. Desbos, P. Jansook, *PharmSciTech*, 2008, **9**, 425-430.
 42. M. P. M. Marques, P. J. Oliveira, A. J. M. Moreno, L. A. E. Batista de Carvalho, *J. Raman Spectrosc.*, 2002, **33**, 778-783.
 43. X. Chen, K. R. Morris, U. J. Griesser, S. R. Byrn, J. G. Stowell, *J. Am. Chem. Soc.*, 2002, **50**, 15012-15019.
 44. L. Wei, P. Sun, S. Nie, W. Pan, *Drug Dev. Ind. Pharm.*, 2005, **31**, 785-794.
 45. O. Planinšek, B. Kovačič, F. Vrečer, *Int. J. Pharm.*, 2011, **406**, 41-48.
 46. *US Pat.*, 7268156, 2007.

TABLE OF CONTENTS ENTRY



Carvedilol polymorph III, with higher melting point and higher dissolution than polymorph II, shows a potential strategy for carvedilol development.